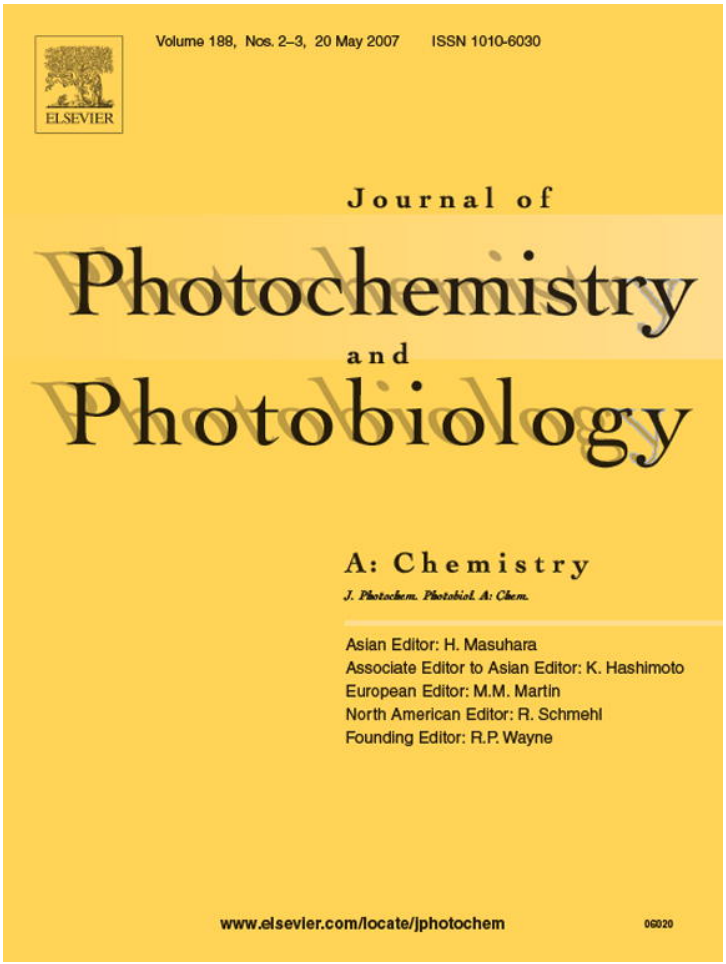

Available online at www.sciencedirect.com
ScienceDirect
Journal of Photochemistry and Photobiology A: Chemistry 188 (2007) 185–191
Journal of Photochemistry and Photobiology A:Chemistry
www.elsevier.com/locate/jphotochem

Characterizing some photophysical, photochemical and photobiological properties of photosensitizing anthraquinones

Laura R. Comini [a], Susana C. Núñez Montoya [a], Martín Sarmiento [b], José L. Cabrera [a], Gustavo A. Argüello [b,*]

[a] *Farmacognosia, Departamento de Farmacia, Facultad de Ciencias Químicas, Universidad Nacional de Córdoba (IMBIV-CONICET), Ciudad Universitaria, 5000 Córdoba, Argentina*
[b] *Departamento de Físico Química, Facultad de Ciencias Químicas, Universidad Nacional de Córdoba (INFIQC-CONICET), Ciudad Universitaria, 5000 Córdoba, Argentina*

Received 9 October 2006; received in revised form 28 November 2006; accepted 6 December 2006
Available online 9 December 2006

Abstract

Some photophysical, photochemical and photobiological properties of nine anthraquinones (AQs) isolated from a phototoxic plant, *Heterophyllaea pustulata*, were studied. The photosensitized generation of superoxide anion radical ($O_2^{\bullet -}$) and singlet molecular oxygen ($^1O_2$) by three of the nine AQs, namely heterophylline, pustuline and 5,5′-bisoranjidiol was evaluated. Whereas the $O_2^{\bullet -}$ production (Type I photosensitization mechanism) was examined in vitro using human leukocyte suspensions and measuring the reduction of NBT, the $^1O_2$ generation (Type II photosensitization mechanism) was studied in an organic solvent through the measurement of the quantum yield of $^1O_2$ (ϕ_Δ). It was established that these three AQs possess photosensitizing properties as do the other AQ derivatives present in this vegetable species, soranjidiol, soranjidiol 1-methyl ether, rubiadin, rubiadin 1-methyl ether, damnacanthal and damnacanthol, acting both by Type I and Type II mechanisms. Furthermore, nordamnacanthal, a species synthesized in the laboratory from one of the natural AQs, showed the highest production of $^1O_2$.

The ability of natural AQs to deactivate the $^1O_2$ generated during the photosensitization process as well as their fluorescence (as competitive mechanisms to the generation of ROS) was studied.

Keywords: Anthraquinones; Photosensitization; ROS; Quenching; Rate constants; *Heterophyllaea pustulata*

Abbreviations: AQs, anthraquinones; $^3O_2$, molecular oxygen; $^1O_2$, singlet molecular oxygen; $O_2^{\bullet -}$, superoxide anion radical; NBT, nitroblue tetrazolium; UV, ultraviolet; UVR, UV radiation; k_r, reactive rate constant for $^1O_2$ quenching; k_q, physical rate constant for $^1O_2$ quenching; ZnTPP, zinc tetraphenylporfine; 9,10-DPA, 9,10-diphenylanthracene; ^{1}H NMR, proton nuclear magnetic resonance spectroscopy; ^{13}C NMR, ^{13}carbon nuclear magnetic resonance spectroscopy; IR, infrared spectroscopy; UV–vis, ultraviolet–visible spectroscopy; MS, mass spectrometry; PN, perinaphthenone (1H-phenalen-1-one); NP, naphthalene; $AlCl_3$, aluminum chloride; $CHCl_3$, chloroform; ROS, reactive oxygen species; ϕ_Δ, quantum yield of singlet oxygen; k_t, total rate constant for $^1O_2$ quenching; TLC, thin-layer chromatography; NH_4OH, ammonium hydroxide; Abs, absorbance; Abs_0, time zero absorbance; S, photosensitizer; Q, quencher; $[Q]$, quencher concentration; τ, $^1O_2$ lifetime in the presence of the quencher; k_d, rate constant for $^1O_2$ quenching for the solvent; τ_0, $^1O_2$ lifetime in the absence of the quencher; ϕ_f, quantum yield of fluorescence; λ_{exc}, exciting wavelength; I_f, fluorescence intensity; I_0, detector's response taken at the maximum of the production-decay curve

* Corresponding author at: Dpto de Físico Química, Medina Allende esq. Haya de La Torre, Ciudad Universitaria, 5000 Córdoba, Argentina.
Tel.: +54 351 4334169; fax: +54 351 4334188.
E-mail address: gaac@fcq.unc.edu.ar (G.A. Argüello).

1010-6030/$ – see front matter © 2006 Elsevier B.V. All rights reserved.
doi:10.1016/j.jphotochem.2006.12.011

1. Introduction

Anthraquinones (AQs) constitute the most numerous group from all the quinones present in the vegetable kingdom [1]. From the species *Heterophyllaea pustulata* Hook. f. (Rubiaceae), popularly known as "cegadera", "ciegadera" or "saruera" [2], the following AQs have been isolated and identified as predominant metabolites: soranjidiol (**1**), soranjidiol 1-methyl ether (**2**), rubiadin (**3**), rubiadin 1-methyl ether (**4**), damnacanthal (**5**), damnacanthol (**6**), heterophylline (**7**), pustuline (**8**) and the bianthraquinone (*S*)-5,5′-bisoranjidiol (**9**) [3,4]. It is important to emphasize that **7**, **8** and **9** constitute new structures, recently described for this family of compounds [4].

We have previously demonstrated that six of the natural AQs (**1**–**6**) possess photosensitizing activity (either Type I or Type II) [5] and therefore they should be involved in the phototoxic effect that *H. pustulata* produces on cattle. This effect is expressed as

dermatitis and blindness (kerato-conjunctivitis), which are due to a typical primary photosensitization reaction [6].

AQs can interact with molecular oxygen in several ways. With the ground state molecule ($^3O_2$), they behave as sensitizers able to produce either the electronically excited molecule ($^1O_2$) through a Type II process or the electronic ground state of the radical anion ($O_2^{\bullet -}$) through a Type I process with variable yields [7–9]. With the electronically excited molecule ($^1O_2$), they tend to deactivate or quench it either producing new substances (reactive quenching) or just releasing the excess energy as heat [10]. We here report the photogeneration of both $O_2^{\bullet -}$ and $^1O_2$ by the new anthraquinones **7**, **8** and **9**. The production of $O_2^{\bullet -}$ (Type I mechanism) was detected and quantified with an indirect relative photobiological method that measures the reduction of Nitroblue Tetrazolium (NBT) by the $O_2^{\bullet -}$ generated within human leukocytes when the AQ is present in the dark and also after continuous UV radiation (290–400 nm or UVR). The ability to generate $^1O_2$ (Type II mechanism) when each AQ is excited by pulsed laser radiation (N_2 laser) was determined by measuring the direct luminescence of the $^1O_2$ generated. In addition to the natural AQs, one derivative purposely devised and synthesized (vide infra), nordamnacanthal (**10**), was evaluated in relation to its $^1O_2$ production. Furthermore, we have analyzed all the natural AQs as quenchers of $^1O_2$. The total (reactive + physical; $k_r + k_q$) deactivation was determined using time resolved infrared luminescence detection. In turn, the chemical contribution to the total quenching was derived from a steady-state relative method that used zinc tetraphenylporfine (ZnTPP) as sensitizer and 9,10-diphenylanthracene (9,10-DPA) as reference ($k_r = 4.2 \times 10^6\ M^{-1}\ s^{-1}$) [11].

In order to obtain a better characterization of these AQs, on account of their involvement on the de-excitation process from the first excited singlet, we have measured the relative fluorescence quantum yields in chloroform solutions as well as the chemical stability during the irradiation process.

2. Materials and methods

2.1. Chemicals

The AQs (Fig. 1) were isolated and purified according to the procedures described previously [3,4]. Whereas the known derivatives (**1**–**6**) were identified by comparison of their spectral data with values reported in the literature [3], the structures of the new AQs (**7**–**9**) were established by analysis of their spectroscopic properties (^{1}H NMR, ^{13}C NMR, IR, UV–vis, MS) [4].

Dextran, Histopaque-1077 and Nitroblue Tetrazolium (NBT) were obtained from Sigma Chemical Co. (St. Louis, MO). Perinaphthenone (1H-phenalen-1-one, PN), zinc tetraphenylporfine (ZnTPP), 9,10-diphenylanthracene (9,10-DPA) and naphthalene (NP) were purchased from Aldrich Chem. Co. Aluminum chloride ($AlCl_3$) and precoated Silica gel 60 plates were from Merck. All the compounds were used as received. A whole set of solvents was distilled prior to use and from them, chloroform ($CHCl_3$) was selected because it dissolves all the studied AQs.

2.2. ROS ($O_2^{\bullet -}$ and $^1O_2$) production and irradiation conditions

A photobiological method, NBT assay, was performed in order to evaluate the $O_2^{\bullet -}$ photogeneration by each AQ under dark and continuous UVR, this last condition was obtained using a deuterium lamp system. An equipment for time-resolved near infrared detection of $^1O_2$ phosphorescence was employed to produce and quantify $^1O_2$ along with its quantum yield (ϕ_Δ), and to determine the constants of total quenching (k_t). The ϕ_Δ was calculated by using a comparative method, in which PN was used as reference photosensitizer ($\phi_\Delta = 0.95 \pm 0.05$) [12]. Both irradiation systems have been described in a previous study [5].

A high-pressure SP 200 Bausch & Lomb mercury light source was used to achieve the steady-state photolysis study and to establish the constants of reactive quenching (k_r). In order to obtain a monochromatic light, the beam from the mercury lamp was passed through a Bausch & Lomb high-intensity monochromator.

2.3. Nordamnacanthal

Nordamnacanthal (**10**) was obtained by demethylation of **5** with $AlCl_3$ [13]. Damnacanthal (1.1 mg) was dissolved in benzene (0.4 ml) and $AlCl_3$ (0.14 g) was added. The solution was placed in a double boiler during 1 h and the reaction was stopped with the addition of water. The organic fraction was further purified by preparative TLC on Silica gel with $CHCl_3$ as mobile phase, where **10** was revealed under UV light with NH_4OH fumes ($R_f = 0.6$). Its chemical identity was confirmed by comparison of their spectroscopic data (UV–vis, IR, MS, ^{1}H NMR) with those previously published in the literature [1].

2.4. $^1O_2$ reactive and total quenching determination

The deactivation of $^1O_2$ by chemical reaction was followed through a comparative steady-state method and using $CHCl_3$ as solvent [10]. The determination of the rate constants (k_r) required continuous irradiation of ZnTPP ($Abs_{532} = 0.289$), used as sensitizer. A known chemical quencher, 9,10-DPA ($k_r = 4.2 \times 10^6\ M^{-1}\ s^{-1}$) was used as reference. The disappearance of both substrate (AQ) and reference (9,10-DPA) was followed through UV–vis spectrophotometry. An UV–vis Hewlett Packard 8453, diode array spectrophotometer with 1 nm resolution was employed. The rate constant, k_r, was obtained from the ratio of the slopes of the linear plots $\ln(Abs_0/Abs)$ *versus irradiation time* for the reference and each AQ. The attainment of total deactivation rate constants of $^1O_2$ by the AQs ($k_t = k_r + k_q$; reactive + physical) was performed with the time resolved infrared luminescence technique [5]. In these measurements, every AQ was used simultaneously as sensitizer and quencher (S = Q) with the sole exception of **4** because its quantum yield for the production of the excited state of oxygen was ($\phi_\Delta = 0.0$) [5]. In this case, PN ($Abs_{337.1} = 0.2$) was the sensitizer.

The method used for the antrhaquinones that act both as sensitizers and quenchers requires the progressive increase in the

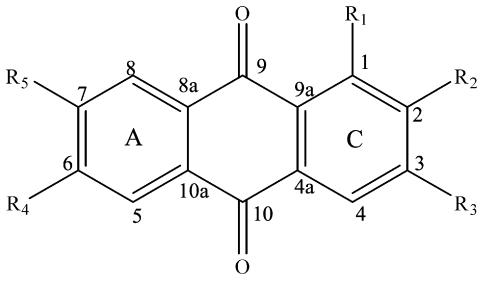

AQs	R_1	R_2	R_3	R_4	R_5
soranjidiol (**1**)	OH	CH_3	H	OH	H
soranjidiol 1-methyl ether (**2**)	OCH_3	CH_3	H	OH	H
rubiadin (**3**)	OH	CH_3	OH	H	H
rubiadin 1-methyl ether (**4**)	OCH_3	CH_3	OH	H	H
damnacanthal (**5**)	OCH_3	CHO	OH	H	H
damnacanthol (**6**)	OCH_3	CH_2-OH	OH	H	H
heterophylline (**7**)	OH	CH_3	H	OH	OCH_3
pustuline (**8**)	H	OH	OCH_3	H	CH_3
nordamnacanthal (**10**)	OH	CHO	OH	H	H

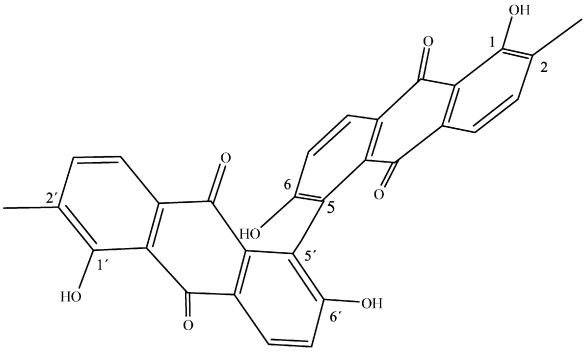

(*S*) -5,5′-bisoranjidiol (**9**)

Fig. 1. Structures of the anthraquinones used in this study.

concentration of AQ following every decay recording, until the luminescence is completely quenched. Every individual $^1O_2$ lifetime was determined by averaging 36 independent decay traces (36 successive laser flashes). Since the concentration of AQ changes negligibly over the reaction period, first-order kinetics results, with an observed rate constant for the decay of $^1O_2$ of $1/\tau$ ($1/\tau = k_d + (k_r + k_q)$ [Q]). This slightly modified Stern–Volmer equation was needed due to the lack of a lifetime measurement free from the presence of the quencher [5]. The slope and intercept, of a plot $1/\tau$ *versus* [*Q*], give values of $(k_r + k_q)$ for the quencher and k_d for the solvent, respectively.

For rubiadin 1-methyl ether (**4**) which does not generate any measurable amount of singlet oxygen, an independent sensitizer was used (PN ($Abs_{337.1} = 0.2$)) and therefore the $^1O_2$ lifetimes were evaluated in the absence (τ_0) and in the presence (τ) of the quencher, and their ratio plotted as a function of AQ concentration using the standard Stern–Volmer treatment (Eq. (1)) [10]:

$$\frac{\tau_0}{\tau} = 1 + k_t \tau_0 [Q] \quad (1)$$

In Eq. (1), $k_t = (k_r + k_q)$ is given by the addition of the respective rate constants depicted in Eqs. (2) and (3):

$$^1O_2 + AQ \xrightarrow{k_q} {}^3O_2 + AQ \quad (2)$$

$$^1O_2 + AQ \xrightarrow{k_r} \text{products} \quad (3)$$

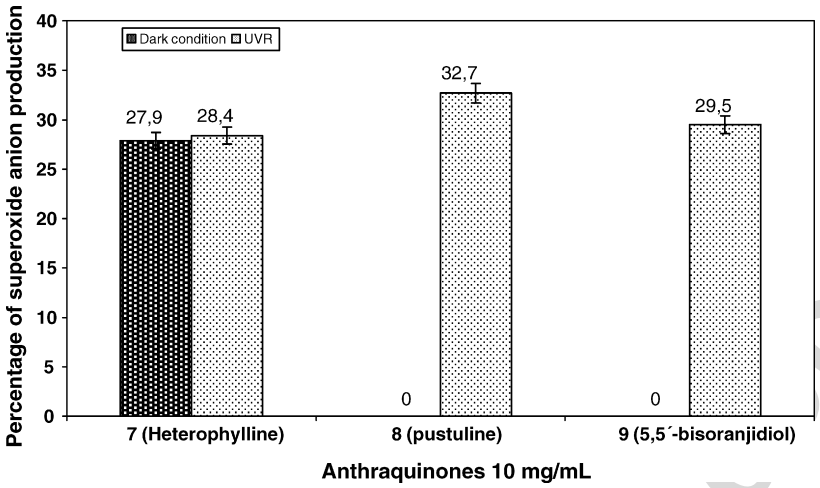

Fig. 2. Stimulation of $O_2^{\bullet -}$ generation in leukocytes by natural AQs (10 μg/mL). Assay of NBT reduction in dark condition and with UV radiation.

2.5. Fluorescence

The relative fluorescence quantum yields (ϕ_f) for the AQs were measured in $CHCl_3$. On the basis of the excitation spectra of each AQ and depending on its excitation wavelength (λ_{exc}), two different references were used: 9,10-DPA ($\lambda_{exc} = 350$ nm, $\phi_f = 1$) [14] for **1**, **3**, **4**, **6**, **7**, **8** and **9** and naphthalene (NP) ($\lambda_{exc} = 270$ nm, $\phi_f = 0.23$) [15] for **2** and **5**.

All the sample solutions were prepared to yield the same absorbance ($A = 0.2$) at the specified λ_{exc} because, in that way, the same number of photons is absorbed for the same irradiating conditions [16].

The emission fluorescence spectra were recorded with a PTI (Photon Technology International) – Quanta master II and the relative quantum yield was evaluated according to

$$\phi_{f(AQs)} = \frac{I_{f(AQs)} \times \phi_{f(Ref)}}{I_{f(Ref)}}$$

The fluorescence intensities (I_f) were recorded at the maximum of emission for both, reference and AQs.

2.6. Photolysis

The photochemical studies were carried out in steady-state conditions by irradiating the AQs dissolved in $CHCl_3$ ($Abs_{337.1} = 0.2$) under two different conditions. Monochromatic light corresponding to the absorption maximum for each AQ was used with one set and the other set of samples was irradiated with the whole output of the lamp. Irradiation times varied between 15 and 7200 s. The course of the reaction was followed by UV–vis spectrophotometry.

3. Results and discussion

3.1. Determination and quantification of ROS ($O_2^{\bullet -}$ and $^1O_2$) for the three new AQs (7, 8 and 9)

The production of $O_2^{\bullet -}$ by each AQ, in the absence and presence of UVR, was measured under aerobic conditions by the NBT assay previously explained. The stimulation of the oxidative metabolism in human leukocytes by **7**, **8** and **9** at 10 μg/mL, in darkness and under irradiation is shown in Fig. 2. Compounds **8** and **9** stimulated $O_2^{\bullet -}$ formation only when they were irradiated, and showed a similar yield. Although **7** showed stimulation to the production of $O_2^{\bullet -}$ in the dark, it did not show photostimulation at 10 μg/mL. Since the oxidative metabolism is dose-dependent [17], we increased the concentration two-fold (20 μg/mL) in order to observe the behavior under UVR. At this higher dose, **7** produced a measurable increase in oxidative stress under dark conditions, which was further intensified by exposition to UVR (Table 1).

The three new AQs generated $^1O_2$ in $CHCl_3$ when they were excited with 337.1 nm radiation. The quantum yield values (ϕ_Δ) listed in Table 2 were derived from the ratio of the slopes of the linear plots I_0 *versus* laser energy (Fig. 3) for each AQ and the reference. Although not all the AQs are shown in Fig. 3, good straight lines for energies below 0.9 mJ/pulse are obtained for them, evidencing that no saturation effects are involved.

In a previous study [5], we showed that the presence of an OH group in the 1-position (α-OH) of the basis structure of the AQ leads to an increase in the singlet oxygen production quantum yield (ϕ_Δ). An inspection of the values of ϕ_Δ for **7** (0.41 ± 0.02) and **8** (0.11 ± 0.01), measured in the present study, shows again that the presence of the OH adjacent to the carbonyl group in the compound **7** notably increases the $^1O_2$ production with respect to

Table 1
Stimulation percentage of $O_2^{\bullet -}$ generation in leucocytes produced by natural AQs

Concentration (μg/mL)	Compound	Dark	UVR
10	heterophylline (**7**)	27.9 ± 3.7	28.4 ± 3.0
	pustuline (**8**)	0.0	32.7 ± 3.9
	5,5′-bisoranjidiol (**9**)	0.0	29.5 ± 2.9
20	heterophylline (**7**)	33.0 ± 5.8	45.7 ± 8.1
	pustuline (**8**)	0.0	54.9 ± 9.4
	5,5′-bisoranjidiol (**9**)	0.0	32.0 ± 6.5

Assay of NBT reduction in dark condition and with UV radiation.

Table 2
Quantum yields for $^1O_2$ generation upon direct 337.1 nm irradiation and quenching rate constants (k_r and k_t) in $CHCl_3$

AQ	ϕ_Δ	Quenching rate constant		
		k_r ($\times 10^5$ M^{-1} s^{-1})	k_t ($\times 10^5$ M^{-1} s^{-1})	ϕ_r (k_r/k_t)
1	0.47 ± 0.04[a]	2.79 ± 0.19	13.40 ± 0.03[a]	0.208
2	0.07 ± 0.01[a]	<0.1	5.72 ± 0.23[a]	0.017
3	0.34 ± 0.04[a]	4.20 ± 0.13	19.35 ± 0.08[a]	0.217
4	0.00[a]	2.62 ± 0.04	10.81 ± 0.02	0.242
5	0.70 ± 0.03[a]	3.81 ± 0.15	3.97 ± 0.16[a]	0.957
6	0.31 ± 0.01[a]	1.89 ± 0.09	6.31 ± 0.19[a]	0.299
7	0.41 ± 0.02	1.01 ± 0.02	6.50 ± 0.02	0.155
8	0.11 ± 0.01	2.15 ± 0.10	2.69 ± 0.03	0.799
9	0.18 ± 0.01	<0.1	5.45 ± 0.13	0.018
10	0.84 ± 0.10			

[a] See Ref. [5].

8. The presence of a hydrogen-bonded carbonyl group could be enhancing the radiationless deactivation processes of the electronically excited singlet state of the AQ, possibly due to the rigidization of the whole structure, which is manifested through the increase in the formation of $^1O_2$.

However, it was observed that AQs without the OH group in 1-position, i.e. damnacanthal (**5**) and damnacanthol (**6**), showed from moderate to important quantum yield values (see Table 2). This observation led us to postulate that the presence of aldehyde and alcohol functional groups in 2-position would be counteracting the absence of the α-OH and would be reverting the lower quantum yields due to the OCH_3 group in 1-position. On the basis of this analysis, it would be interesting to determine the ϕ_Δ for the R1 = OH, R2 = CHO derivative (nordamnacanthal, **10**). Therefore, we looked for a convenient synthesis of **10** and we succeeded in using a biosynthetic path starting from **5** as discussed in Section 2.3. Fig. 3 shows the behavior for nordamnacanthal (**10**) in $CHCl_3$. The closeness in the slope with that of the reference immediately suggests a quantum yield for the production of singlet oxygen close to unity. Table 2 summarizes the values of ϕ_Δ for the new AQs and it is readily seen that **10** shows the highest quantum yield for all the AQs studied.

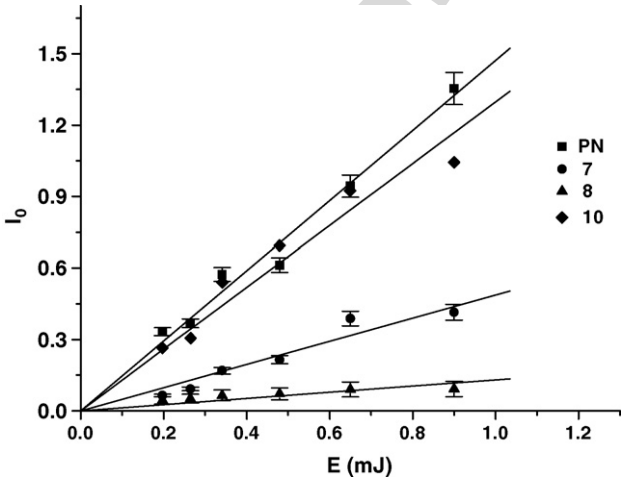

Fig. 3. Laser fluence dependence of the amplitude at zero-time I_0 of the $^1O_2$ phosphorescence signal in $CHCl_3$ for PN, **7**, **8** and **10**.

3.2. $^1O_2$ reactive and total quenching determination

The reactive rate constant (k_r) for each AQ was determined using the comparative steady-state method described. Fig. 4 shows the linear plot ln (Abs_0/Abs) *versus* irradiation time for the reference used (9,10-DPA) and one particular AQ, namely, damnacanthal (**5**). In all cases, good straight lines were obtained. The absolute values of k_r are modest (Table 2); they do not correspond to particularly good reactive quenchers. Although no attempts were made to study the products of the reaction between the AQs and $^1O_2$, it is accepted that the initial attack of the oxygen molecule should be on a double bond in the molecule [18] to give rise either to a hydroperoxide or an endoperoxide. Being so, there are several possibilities with every AQ and therefore it is difficult to give a trend in the absolute values of the quenching rate constants as was done for the variation in quantum yields [5].

We have also measured the total quenching of the $^1O_2$ emission (k_t), with the time resolved system for the new AQs. Fig. 5 corresponds to the plot of $1/\tau$ *versus* [*Q*] for **7** in a typical experiment. In addition, the k_t of **4** was evaluated according to a simple Stern–Volmer treatment; the plot of τ_0/τ *versus* [*Q*] for this AQ is shown in Fig. 6.

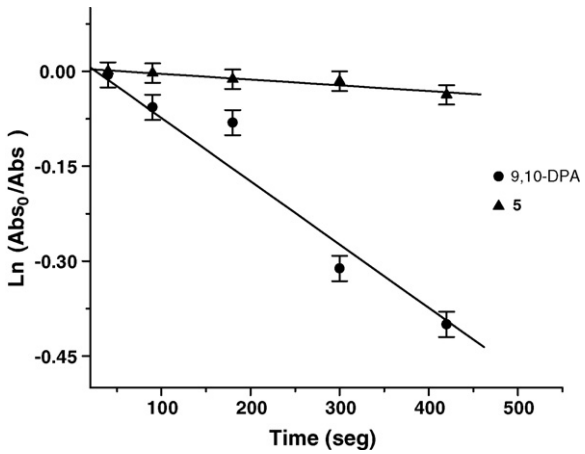

Fig. 4. Reactive quenching rate constant derived for DPA and **5**.

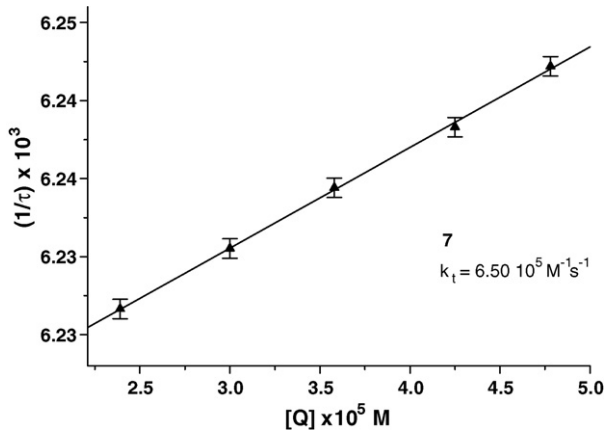

Fig. 5. Total quenching rate constant derived for **7**.

The absolute values for the total rate constants are also listed in Table 2. An inspection reveals that the great majority of the AQs are poor or moderate quenchers. While the overall constants do not change dramatically between different partners, some of them show a degree of self-protection, defined as (k_r/k_t), [19] against photooxidation (Table 2). Particularly, **2** and **9** present a very good self-protection ratio mainly due to very low reactive rate constants. Within the same order of magnitude for k_t, **5** and **8** present the worst case for self-protection with a ratio close to unity.

3.3. Fluorescence and steady-state photolysis

Frequently, it is experimentally observed that fluorescence spectra and ϕ_f in liquid solutions are independent of the wavelength of exciting light [20]. For these reasons, the excitation wavelength used to excite the AQs was not exactly the same as those of the references but close. The results obtained (see Table 3) show very low fluorescence yields (around 10^{-2} to 10^{-4}) for most of the AQs and a particular one (**6**) whose quantum yield is below our detection limit.

Through the observation of the absorption UV spectra and their variation with time, we concluded that the decomposition

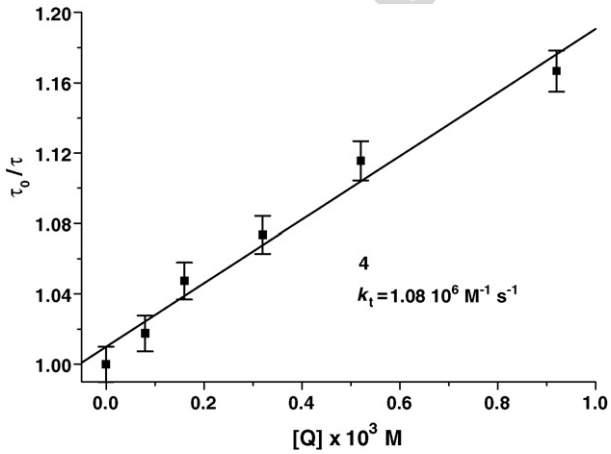

Fig. 6. Stern–Volmer plot for the quenching of **4**.

Table 3
Quantum yields of fluorescence of the natural AQs

AQ	Reference	λ_{exc}	ϕ_f
1	9,10 DPA	395.5	0.0050 ± 0.0002
2	Naphthalene	276	0.0145 ± 0.0009
3	9,10 DPA	376	0.0180 ± 0.0010
4	9,10 DPA	376	0.0011 ± 0.0001
5	Naphthalene	276	0.0202 ± 0.0002
6	9,10 DPA		–
7	9,10 DPA	395.5	0.0052 ± 0.0003
8	9,10 DPA	374	0.0076 ± 0.0004
9	9,10 DPA	395.5	0.0008 ± 0.0001

of the illuminated AQs is negligible within the total irradiation time.

4. Conclusions

The newly studied AQs (**7**–**9**) photostimulate the oxidative stress in leukocytes mainly due to an increase in the production of $O_2^{\bullet -}$. They also produce $^1O_2$ when irradiated, **7** being the most effective with a quantum yield ($\phi_\Delta = 0.41 \pm 0.02$). In general, these substances behave similarly to the other AQs isolated from *H. pustulata* [5]. As a general statement all the AQs are poor or moderate singlet oxygen quenchers.

Acknowledgements

L.R.C. and S.C.N.M. acknowledge research fellowship received from CONICET. Support for this work came from SeCyT-UNC, FONCYT and Agencia Córdoba Ciencia.

References

[1] R. Wijnsma, R. Verpoorte, in: W. Herz, H. Grisebach, G.W. Kirby, Ch. Tamm (Eds.), Prog. Chem. Org. Nat. Prod., vol. 49, Springer-Verlag, Wien, 1986, pp. 79–149.
[2] N.M. Bacigalupo, in: A.L. Cabrera (Ed.), Flora de la Provincia de Jujuy, Colección Científica INTA, tomo III, parte IX, INTA, Buenos Aires, 1993, pp. 375–380.
[3] S.C. Núñez Montoya, A.M. Agnese, C. Pérez, I.N. Tiraboschi, J.L. Cabrera, Phytomedicine 10 (2003) 569–574.
[4] S.C. Núñez Montoya, A.M. Agnese, J.L. Cabrera, J. Nat. Prod. 69 (2006) 801–803.
[5] S.C. Núñez Montoya, L.R. Comini, M. Sarmiento, C. Becerra, I. Albesa, G.A. Argüello, J.L. Cabrera, J. Photochem. Photobiol. B: Biol. 78 (2005) 77–83.
[6] E.W. Hansen, C.A. Martiarena, Rev. Invest. Agropecuarias (INTA) 4 (1967) 81–113.
[7] K. Gollnick, S. Held, D.O. Mártire, S.E. Braslavsky, J. Photochem. Photobiol. A: Chem. 69 (1992) 155–165.
[8] K.J. Reszka, P. Bilski, C.F. Chignell, J.A. Hartley, N. Khan, R.L. Souhami, A.J. Mendonca, J.W. Lown, J. Photochem. Photobiol. B: Biol. 15 (1992) 317–335.
[9] L.-Y. Zang, B.R. Misra, H.P. Misra, Photochem. Photobiol. 56 (1992) 453–462.
[10] I. Gutiérrez, S.G. Bertolotti, M.A. Biasutti, A.T. Soltermann, N.A. García, Can. J. Chem. 75 (1997) 423–428.
[11] F. Wilkinson, W.P. Helman, A.B. Ross, J. Phys. Chem. Ref. Data 24 (1995) 663–1022.

[12] R. Schmidt, C. Tanielian, R. Dunsbach, C. Wolff, J. Photochem. Photobiol. A: Chem. 79 (1994) 11–17.
[13] S. Nonomura, Pharm. Soc. Jpn. 75 (1955) 219–221.
[14] E.J. Bowen, J. Sahu, in: L.J. Heidt, R.S. Livingston, E. Rabinowitch, F. Daniels (Eds.), Photochemistry in the Liquid and Solid State, 1st ed., John Wiley & Sons Inc., New York, 1960, pp. 55–61.
[15] H. Du, R.A. Fuh, J. Li, A. Corkan, J.S. Lindsey, Photochem. Photobiol. 68 (1998) 141–142.
[16] I.E. Kochevar, R.W. Redmond, in: J.N. Abelson, M.I. Simon (Eds.), Meth. Enzymol., vol. 319, Academic Press, USA, 2000, pp. 20–28.
[17] C. Becerra, I. Albesa, A.J. Eraso, Biochem. Biophys. Res. Commun. 285 (2001) 414–418.
[18] T. Matsuura, H. Matsushima, R. Nakashima, Tetrahedron 26 (1970) 435–443.
[19] N.A. García, S.N. Criado, W.A. Massad, in: E. Silva, A.M. Eduards (Eds.), Comprehensive Series in Photosciences, Elsevier Science Publishers, 2006, Chap. 4, pp. 61–82.
[20] J.G. Calvert, J.N. Pitts Jr., Photochemistry, 1st ed., John Wiley & Sons Inc., New York, 1966.